XLIII CILAMCE
21–25, November, 2022
FOZ DO IGUAÇU – PR – BRAZIL

PARAMETRIC OPTIMIZATION OF QUARTER VEHICLE SUSPENSION MODEL BY RESPONSE MAP TECHNIQUE

Leonardo da Costa Rodrigues Ferreira[1], Suzana M. Avila[2], Marcus V. G. de Morais[3]

[1,3]*Depto. Mechanical Engineering, University of Brasilia, Campus Darcy*
Brasília/DF
rodrigues.ferreira@aluno.unb.br, mvmorais@unb.br
[2]*Depto. Automotive Engineering, University of Brasília, Campus Gama*
avilas@unb.br
Brasília/DF

Abstract. This work aims to set the suspension optimal parameters of a quarter vehicle model, using an exhaustive parametric optimization technique. The objective function minimizes sprung mass rms acceleration considering a Gaussian white noise road profile for a fixed sprung/unsprung mass ratio with different control strategies for a semi-active suspension system.
Keywords: Semi-active suspension, 1/4 vehicle, Skyhook

1 Introduction

The ROTA 2030 initiative is a Brazilian state-funded program that provides advances on the automotive technologies employed in the country. One of its focuses is to develop automotive control systems to improve the safety of commercial vehicles. Ride comfort and handling are important qualities for car passengers experience and security.

The suspension vehicle model is exhaustively studied in the literature [1] [2]. Random vibration road surface profiles are used to determine acceleration levels [3] [4]. Gillesp [1] presents some design criteria to set the suspension parameters of a urban vehicle. These design criteria are developed by a parametric analysis of the acceleration transfer functions of a quarter vehicle model.

This work aims to set the suspension optimal parameters of a quarter vehicle model, using an exhaustive parametric optimization technique. The objective function minimizes sprung mass rms acceleration considering a Gaussian white noise road profile for a fixed sprung/unsprung mass ratio with different control strategies for a semi-active suspension system.

2 1/4 vehicle semi-active and methodology

The quarter vehicle model is composed of a tire, which connects to the road, and a mass above it suspended by a spring and a damper. The tire is represented by a mass hanging on top of a spring. The mathematical model thus becomes

$$\begin{bmatrix} M_s & 0 \\ 0 & M_u \end{bmatrix} \cdot \begin{bmatrix} \ddot{x}_s \\ \ddot{x}_u \end{bmatrix} + \begin{bmatrix} c_s & -c_s \\ -c_s & c_s \end{bmatrix} \cdot \begin{bmatrix} \dot{x}_s \\ \dot{x}_u \end{bmatrix} + \begin{bmatrix} k_s & -k_s \\ -k_s & k_s + k_u \end{bmatrix} \cdot \begin{bmatrix} x_s \\ x_u \end{bmatrix} = \begin{bmatrix} 0 \\ z \cdot k_u \end{bmatrix} \tag{1}$$

where k denotes the spring stiffness, c the damper constant, M the mass, z the road profile and x the position of the masses. In cases where there are more than one spring or mass, the subscript denotes which one is being referred with U being unsprung and S being sprung. The variables x and z are both time-dependents, while c_s is time-dependent if a semi-active suspension is being employed. Since z is a random value that follows a statistical distribution, this equation is a stochastic differential equation. Hernandes and Spigler [6] lay out numerical solution methods for such equations. While implicit methods are demonstrated, they become cumbersome to implement

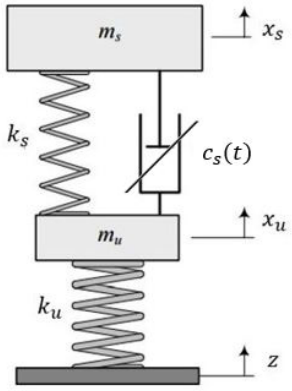

Figure 1. 1/4 vehicle model for a semi-active suspension. Reproduced from Melo [5].

in the semi-active model, where complicated rules are used to determine the value of c_s. As such, they will not be used in either model for consistency. The simplest explicit method is the Euler Forward scheme, which will be chosen.

In the system with a passive damper, the equation can also be analytically solved in the frequency domain by the method described by Inman [7], with examples of this specific system by Gillesp [1]. This analytical solution will be used to validate the numerical model in the passive damper system. The relationship between suspended mass gain and the system parameters as a function of a frequency ω is laid out in equation (2), while the same relationship for the unsprung mass is in equation (3). All coefficients in the equation are made dimensionless by division by the suspended mass term, with ξ being the ratio between the unsprung and sprung masses. Dimensionless terms which are also present in equation (1) in a dimensional form are denoted by an sprung case to help differentiate them.

$$H_1(\omega) = \frac{K_s \cdot K_u + j \cdot (K_u \cdot C_s \cdot \omega)}{R(\omega)} \tag{2}$$

$$H_2(\omega) = \frac{K_s \cdot K_u + j \cdot (K_u \cdot C_s \cdot \omega) - \omega^2 \cdot K_u}{R(\omega)} \tag{3}$$

where R is the term in equation (4).

$$R(\omega) = \xi \cdot \omega^4 - (K_u + K_s \cdot \xi + K_s) \cdot \omega^2 + K_s \cdot K_u + j \cdot (K_u \cdot C \cdot \omega - (1 + \xi) \cdot C \cdot \omega^3) \tag{4}$$

The two properties which will be analyzed are the Root Mean Square (RMS) of the sprung mass movement and the roadhold. The RMS of a property such as the gain subject to a white noise input is defined in [1] as the integral of the square of the absolute of said property in the frequency domain, as shown in (5).

$$RMS(H_x) = S \int_0^\infty |H_x(\omega)|^2 d\omega \tag{5}$$

where S is the spectral density of the white noise which the system was subject to. [8] shows the use of this metric by setting the minimization of it as a design objective. This is, in practical terms, declaring that the system must seek the most comfortable ride possible by minimizing the vibrations felt by the passenger given a random road profile. This is formally declared as the relationship in equation (6).

$$f_1 = \min(RMS(H_1(K, C))) \tag{6}$$

where f_1 is the objective function and K and C take all possible values in in the search space.

The Roadhold property is defined in [9] as the difference in height of the unsprung mass and the height of the road profile, as a ratio of the height of the road profile itself. This leads to the term in equation (7). Since the magnitude of the height of the unsprung mass divided by that of the road profile is simply the gain, it also leads to the second form shown in equation (7).

$$rh(\omega) = \frac{x_u - z}{z} = H_2(\omega) - 1 \tag{7}$$

where rh is the value of the Roadhold. The way this property manifests itself on the real system is that, the higher the Roadhold is, the less normal force is exerted on the tires . Since a high gain means there's less normal force, it also means there's less grip on the tires, which puts the vehicle at a greater risk of sliding. As such, it is both a measure of how safe a vehicle is and how capable it is of maintaining contact in extreme situations. Since it is useful to minimize it for every frequency, the relationship shown in equation (8) is used to determine how good a vehicle is at this criteria. It measures which combination of properties in the search space lead to the lowest peak in the Roadhold measurement, thus seeking the system that is the safest in it's most extreme scenario.

$$f_2 = \min(\max(rh(H_2(K, C, \omega)))) \tag{8}$$

While the equations for the gain were already defined for the analytical solutions, the equations that are being solved numerically are done so in the time domain. There is a need to take them to the frequency domain in order to evaluate the two criteria proposed. This will be accomplished by performing the Fourier Transform of the position vectors.

Since the road profile is random, there is no guarantee that a certain result isn't an outlier. To minimize the effects of randomness on the final results, each scenario was solved in the time domain multiple times with a different random road profile, and the average of the Fourier transforms was used.

Even with the averaging process weeding out values too far from the expected real value, the transform is still very noisy, with sudden oscillations and discontinuities in its derivatives. Another treatment is applied, a low pass filter which smooths out the results. This process is done so the final curve more closely resembles the expected behavior of the system, for the wild swings observed are simply an artifact of the random process not being ran for long enough for the values in each bin to be more precisely determined.

For the semi-active systems, c_s is a function of time. What value it assumes is a matter of what control strategy is chosen. Two strategies will be contemplated in the present paper: The Skyhook and Groundhook strategies. These are control strategies which attempt to make the real system emulate the behavior of their namesake systems. The Skyhook system is a 1/4 vehicle model where a damper links the sprung mass with a fixed surface. The Groundhook system is analogous, but it instead has a damper linking the unsprung mass to such surface.

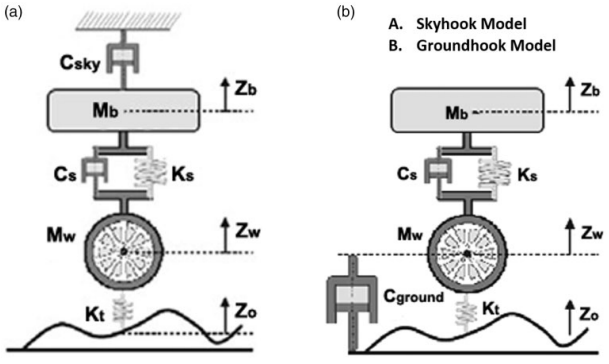

Figure 2. Skyhook and Groundhook systems. Reproduced from [10].

Equation (9) is how the damping coefficient is calculated when employing the Skyhook model, and equation (10) for the Groundhook. These equations are based on the model exposed in [10], with the difference that instead of an on-off switch control scheme they are allowed to continuously vary inside the bounds later set.

$$C = C_{sky} \cdot (\frac{\dot{x}_s}{\dot{x}_s - \dot{x}_u}) \tag{9}$$

$$C = C_{ground} \cdot (\frac{\dot{x}_u}{\dot{x}_u - \dot{x}_s}) \tag{10}$$

It will be assumed that there is instant knowledge of the speed of the masses by the controller. This is not true on a real system, but this method allows for a baseline performance to be established.

3 Parameters and results

The equations were solved numerically with a time-step of 10^{-4}. The road profile used was that of a white Gaussian noise. The sprung mass was set as 250 kg, while the unsprung was set as 25 kg. The tire stiffness was represented by a spring of 10^5 kN·m. The suspension spring and damper were left as free parameters in which the response map would be built upon.

For the semi-active systems, there was the need to choose how the damping coefficient limits would be implemented. Initially, a simple ceiling of 150% and a floor of 50% of the nominal damping coefficient value were chosen. This was done in order to have a consistent rule that could be translated to all points in the domain regardless of the different magnitudes, as opposed to a rule which anchored the extremes at constant values.

One pair of parameters which were harder to determine were the simulation time and number of samples ran for a single point. To determine the least computationally intensive method that still delivered an acceptable solution, the numerical solution was ran multiple times on 9 different points in the solution space for each combination of simulation time and number of samples. The points were all possible combinations of 1e3, 1e4 and 1e5 for both the spring stiffness and and damping coefficient, each ran 60 times. The point which obtained the highest measured value of standard deviation in comparison to its mean for each combination for was selected for comparison. The criteria evaluated were the RMS, roadhold and frequency of peak response, but since in every single test the greatest deviation was found in the RMS only the results for it will be shown. The results for the passive damper configuration are in table (1).

Table 1. Standard deviations in proportion to the mean value for the most critical case in each test in the passive regime.

Simulation time	50 s	150 s	600 s
3 runs	33,67 %	17,43 %	13,02 %
7 runs	24,09 %	20,69 %	8,07 %
11 runs	27,22 %	18,13 %	7,53 %
20 runs	23,11 %	18,24 %	7,71 %

As the data shows, both longer simulation times and more tests lead to a lower variation among the results in the same point, with greater sensibility with regards to the simulation time. A Kolmogorov-Smirnov test failed to reject the hypothesis that the results are normally distributed. As such, the 95% confidence interval is roughly twice the reported standard deviation. For this interval to be less than 20%, the minimal run time has to be of 600s and the minimal amount of runs has to be 7. However, the gains after that are not proportional to the increased computational time. The best cost benefit becomes, then, to run 7 cases with 600 s for each one. If greater precision is deemed necessary, it is better to increase the run time rather than run more cases.

For the semi-active cases, the results were mixed. The Skyhook model obtained 8% of the average as the standard deviation with the chosen parameters, but the Groundhook obtained 18%. This is not an adequate value, which prompted the evaluation with different parameters. Since the table (1) suggests the best cost-benefit lies in increasing the simulation time, another battery was ran with the parameters of 7 tests and 1200 seconds. This resulted in a standard deviation of 11% for the Groundhook model. This was considered enough and it was thereafter calculated with said parameters. The results are also visible in table (2).

Table 2. Standard deviations in proportion to the mean value for the most critical case in the semi-active regime for 7 tests.

Groundhook - 600s	Skyhook - 600s	Groundhook - 1200s
18,14 %	8,14 %	11,30 %

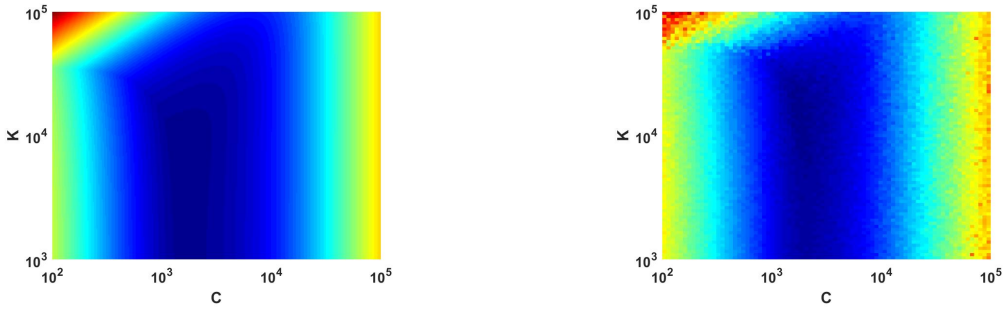

Figure 3. Comparison between the analytical and numerical results for the Roadhold metric, top view, analytical and numerical solutions respectively.

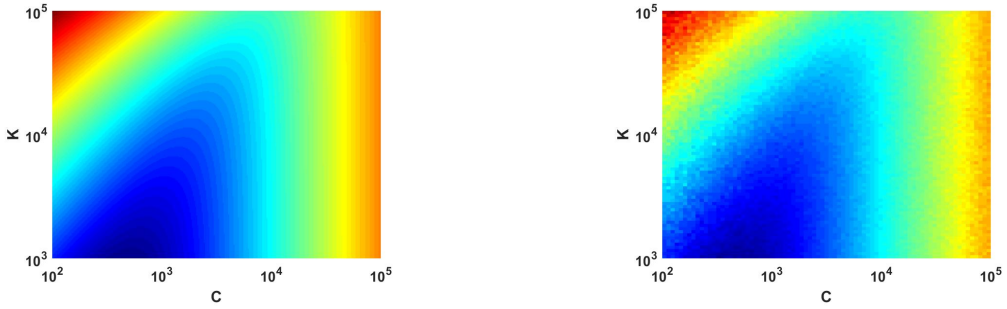

Figure 4. Comparison between the analytical and numerical results for the RMS metric, top view, analytical and numerical solutions respectively.

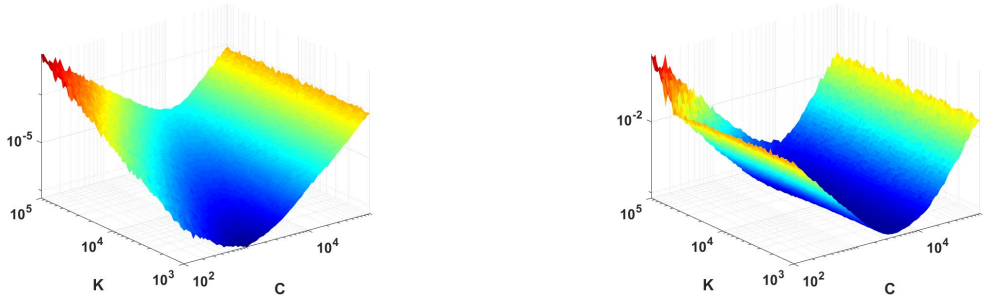

Figure 5. Results for the numerical Groundhook system, isometric view, RMS and Roadhold metrics respectively.

Table 3. Value for the point of minimum in each case, as a percentage of the passive case with the same parameters.

Test	RMS	Roadhold
Passive	100%	100%
Skyhook	77,0%	96,9%
Groundhook	520%	86,6%

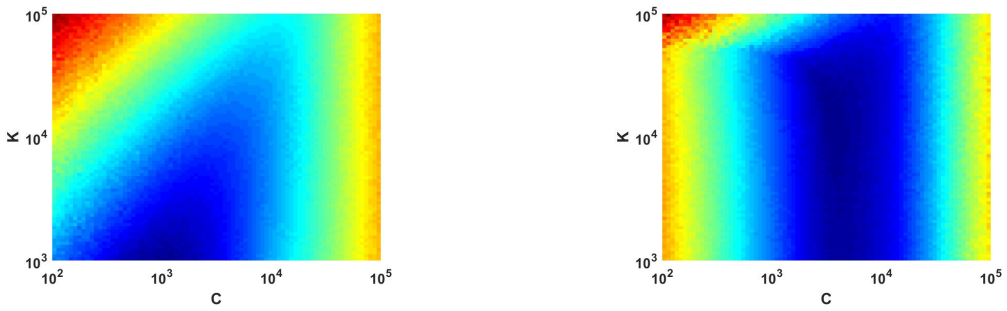

Figure 6. Results for the numerical Groundhook system, top view, RMS and Roadhold metrics respectively.

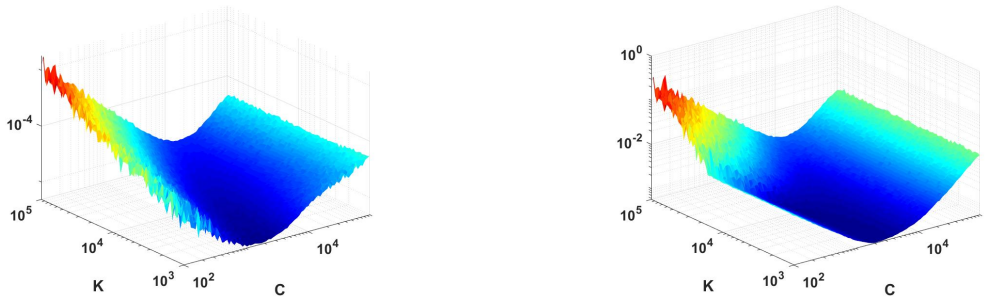

Figure 7. Results for the numerical Skyhook system, isometric view, RMS and Roadhold metrics respectively.

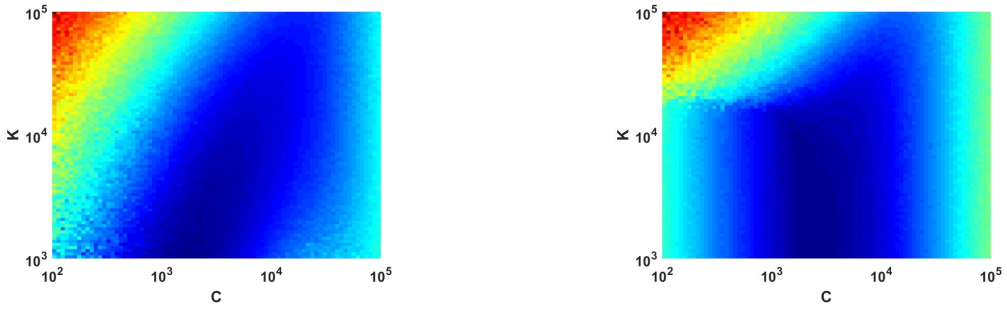

Figure 8. Results for the numerical Skyhook system, top view, RMS and Roadhold metrics respectively.

Table 4. Position for the point of minimum in each case.

Test	RMS				Roadhold			
Skyhook	K:	3360	C:	100	K:	8858	C:	7847
Groundhook	K:	5455	C:	100	K:	9712	C:	6092

The solution was calculated with both the numerical and analytical methodologies in the passive system. The results are in figures (3) and (4). For the system with a semi-active damper, only the numerical simulation was ran. The results for the Skyhook control method are in figures (5) and (6), and for the Groundhook control method are in figures (7) and (8). Table (4) shows a comparison between the lowest values for the semi-active systems compared to the passive system.

The solution of the system with a passive damper successfully demonstrated the behavior of the system with respect to the RMS and Roadhold properties when the values of k_s and c_s are modified. A local minimum for the Roadhold criteria was identified in the passive system inside the studied space, while the RMS showed that a local minimum, if it exists, lies in very small values of spring stiffness and damper coefficients.

The results show the same shape and relative magnitudes, with the main difference being that the numerical solution has 'fuzzy' borders, due to the randomness that the results bring.

The Groundhook system showed a similar geometry to the overall system in broader terms, but with certain differences when looked at closely. Compared to the passive system, in the RMS metric the area which showed a minimum occupied a much broader region, and was slightly shifted to the right, occurring at greater damping coefficients. In the Roadhold metric, there was a shrinkage of the low value region, with regions of high spring constants losing comparative performance. There was a slight gain at low spring and damping coefficient values. However, when the raw values are observed, it is perceived that the system showed an improvement in the Roadhold, with stark regressions in the RMS.

The Skyhook system was more similar to the passive system, with the main difference being that the system was slightly shifted so that the minimum values occurred at greater damping coefficient values. Overall, there was a gain in absolute performance in both the comfort and handling characteristics of the vehicle when compared to the passive system.

Both systems showed improvements. The results for the active suspension system developed by Shirahatti et al [8] showed better performance gains on the same metrics, which is coherent with the expectations that an active suspension will outperform a semi-active one. The Skyhook system presented better performance in the RMS, while the Groundhook presented better performance in the Roadhold criteria.

4 Conclusion and perspectives

It was possible to obtain gains in ride comfort and handling for a vehicle by using a semi-active control methodology. The benefits were greater with the Skyhook approach, but both methodologies showed positive results in their expected niche when compared to the passive approach, with the Skyhook being a ride comfort oriented system and the Groundhook a handling oriented one.

Future studies can be done on more modern control techniques, such as PID controlled systems. Furthermore, different lower and upper bounds for the semi-active control systems can be explored to attempt to obtain better results and to study the impact of increasing or decreasing the values that may be reached by the damper in the vehicle performance. Another point of interest is how the system behaves when additional requirements are imposed, such as the gain requirements for the octave bands which were dealt with by Shirahatti et al [8].

Authorship statement. The authors hereby confirm that they are the sole liable persons responsible for the authorship of this work, and that all material that has been herein included as part of the present paper is either the property (and authorship) of the authors, or has the permission of the owners to be included here.

References

[1] T. D. Gillespie. *Fundamentals of Vehicle Dynamics*, 1992.

[2] R. G. . C. A.A. *Road Vehicle Dynamics: Fundamentals and Modeling with MATLAB®*. CRC Press, 2nd edition, 2020.

[3] R. S. Barbosa. Vehicle dynamic response due to pavement roughness. *Journal of the Brazilian Society of Mechanical Sciences and Engineering*, pp. 302–307, 2011.

[4] ISO 8608:2016. Mechanical vibration — Road surface profiles — Reporting of measured data. Standard, International Organization for Standardization, Geneva, CH, 2016.

[5] M. A. Melo. Análise comparativa de estratégias para suspensão semiativa em um modelo de 1/4 de veículo, 2017.

[6] D. Hernandez and R. Spigler. A -stability of runge-kutta methods for systems with additive noise. *BIT*, vol. 32, pp. 620–633, 1992.

[7] D. J. Inman. Engineering vibration, 2013.

[8] A. Shirahatti, P. Prasad, P. Panzade, and M. Kulkarni. Optimal design of passenger car suspension for ride and road holding. *Journal of the Brazilian Society of Mechanical Sciences and Engineering [online]*, vol. 30, pp. 66–76, 2009.

[9] P. C. Gomes and de M. V. G. Morais. Parametric optimization of tmd inerter for vibration control of vehicle suspension, 2021.

[10] H. B and E. M. *Chassis handbook*. 1 edition, 2011.